

Figure S1. *Pbx1* and *Hox11^{aadd}* do not regulate patterning of distal or proximal superstructures, respectively. (A, A') Sagittal sections through the humeri of *Hox11^{aadd}* mutant and control embryos at E13.5 that were stained against SOX9 and COL2A1. (B, B') Sagittal sections through the elbows of *Pbx1* mutant and control embryos at E13.5 that were crossed to *ScxGFP* transgenic mice and stained against SOX9. Whereas *HoxA11* and *HoxD11* regulated the spatial organization of distal olecranon precursors, organization of the proximal DT precursors was unaffected in *Hox11^{aadd}* compound mutants (A, A'). Conversely, whereas *Pbx1* regulated the spatial organization of proximal DT precursors, organization of the distal olecranon precursors was unaffected in *Pbx1^{null}* mutants (B, B'). Scale bars: 100 μ m.

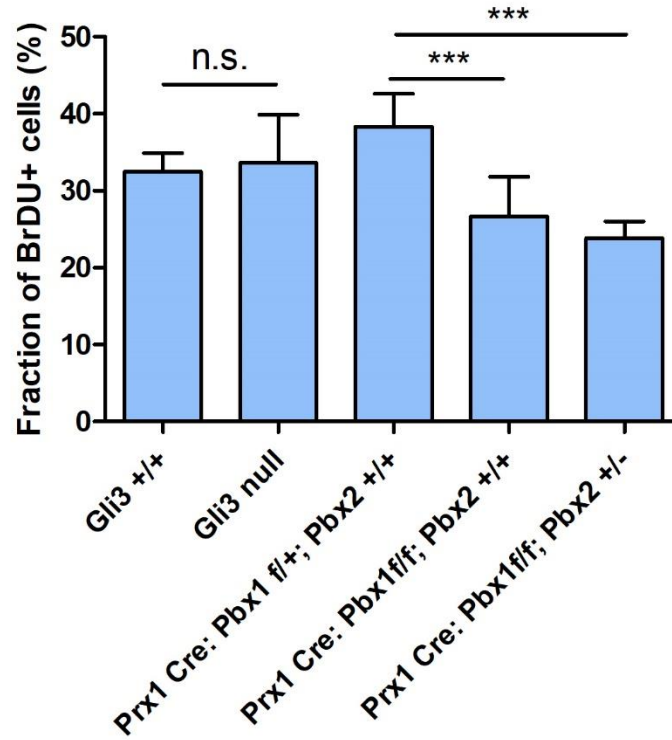





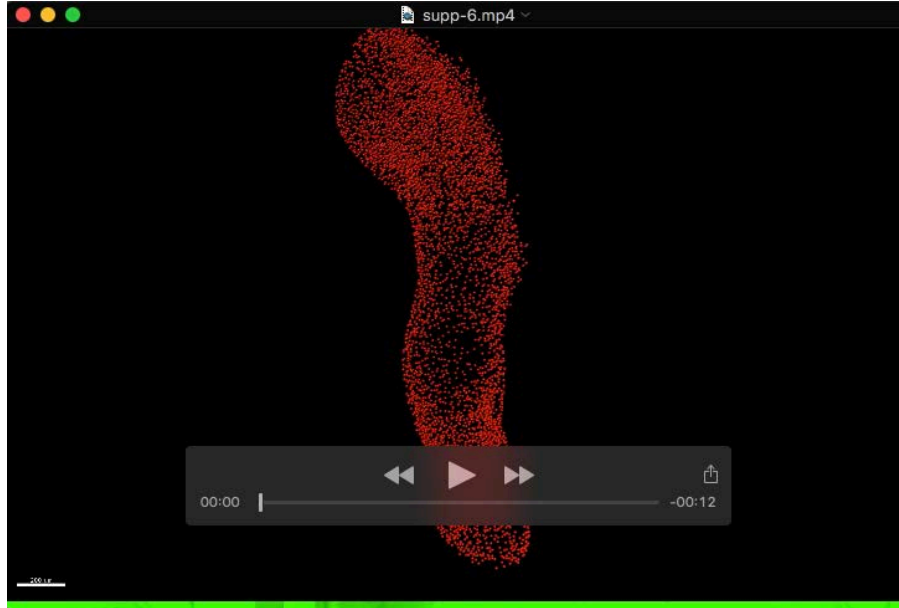


Figure S2. Quantification and comparison of proliferating cells among proximal humeral superstructure precursors in *Gli3* and *Prx-Cre:Pbx1;Pbx2* control and mutant embryos. Paraffin sections taken from E13.5 *Gli3* and *Prx1-Cre;Pbx1;Pbx2* control and mutant forelimbs were immunostained for BrdU. The number of total *Sox9*⁺ and *Sox9*⁺/BrdU⁺ cells were counted in the region of the greater and deltoid tuberosity and the fractions of proliferating cells were calculated for both control and mutant embryos ($n \geq 6$). Whereas proliferation in both *Prx1-Cre;Pbx1^{flxed}* and *Prx1-Cre;Pbx1^{flxed};Pbx2^{het}* mutant embryos was significantly decreased, *Gli3^{null}* embryos did not display significant changes in proliferation compared to control embryos. Statistical significance was determined as $p \leq 0.05$.

Table S1. Quantification of *Gli3^{null}* morphological variations within the deltoid tuberosity, patella and tibia.

Age (n)	Deltoid tuberosity		Patella			Tibia
	Severe/detached	Mild/dysplastic	Absent	Smaller	Deformed	Absent
E15.5 (4)	3/4	1/4	4/4	0/4	0/4	4/4
E17.5 (8)	3/8	5/8	0/4	5/8	3/8	8/8
						

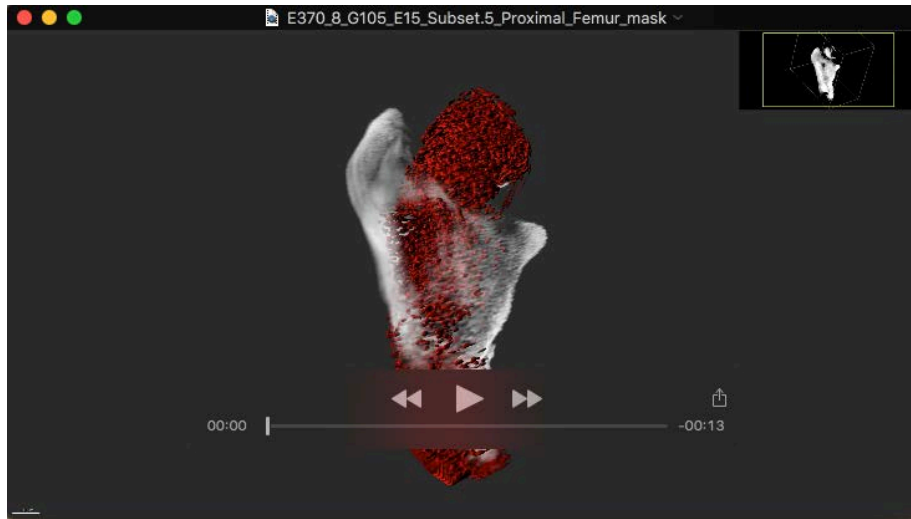
Deltoid tuberosity morphologies were divided into two categories, namely severe or mild dysplasia. Detached deltoid tuberosity was categorized as severe phenotype. Patella morphologies were divided into three categories, namely absent, smaller or deformed. The tibia was absent in all *Gli3* mutant embryos.



Movie 1. *Sox9*⁺/*Scx*⁺ progenitors contribute extensively to humeral morphology. This movie shows a three-dimensional (3D) reconstruction of a humerus and various protruding superstructures. Reconstruction was made from stacked images of E14.5 forelimbs from *Sox9-Cre*^{ER}-*tdTomato* transgenic embryos using Arivis Vision4D (Arivis) and Imaris (Bitplane) software. Forelimb was additionally stained against COL2A1 to label the outer surface of the long bone. Whereas first-wave *Sox9*⁺ progenitors were labeled by tdTomato, the secondary wave of *Sox9*⁺/*Scx*⁺ progenitors remained tdTomato-negative and contributed exclusively to superstructure formation, including bone eminences such as greater, lesser and deltoid tuberosities and various condyles, such as distal, medial and lateral humeral epicondyles.



Movie 2. *Sox9*⁺/*Scx*⁺ progenitors contribute extensively to elbow morphology. This movie shows a 3D reconstruction of the elbow and various protruding superstructures. Reconstruction was made from stacked images of E15.5 forelimbs from *Col2a1-Cre*^{ER}-*tdTomato* transgenic embryos using Arivis Vision4D (Arivis) and Imaris (Bitplane) software. Forelimb was additionally stained against COL2A1 to label the outer surface of the long bone. Whereas first-wave *Sox9*⁺ progenitors were labeled by tdTomato, the secondary wave of *Sox9*⁺/*Scx*⁺ progenitors remained tdTomato-negative and contributed exclusively to superstructure formation, including protrusions such as the olecranon and various condyles, such as distal, medial and lateral humeral epicondyles.



Movie 3. *Sox9*⁺/*Scx*⁺ progenitors contribute extensively to femoral morphology. This movie shows a 3D reconstruction of the proximal femur and various protruding superstructures. Reconstruction was made from stacked images of E15.5 hindlimbs from *Col2a1-Cre^{ER}-tdTomato* transgenic embryos using Arivis Vision4D (Arivis) and Imaris (Bitplane) software. Hindlimb was additionally stained against COL2A1 to label the outer surface of the long bone. Whereas first-wave *Sox9*⁺ progenitors were labeled by tdTomato, the secondary wave of *Sox9*⁺/*Scx*⁺ progenitors remained tdTomato-negative and contributed exclusively to superstructure formation, including bone eminences such as the greater, lesser and third trochanters.